Benzodiazepine Receptor Distribution in Severe Intractable Tinnitus

Aditya Daftary,[1] Abraham Shulman,[3] Arnold M. Strashun,[2] Christopher Gottschalk,[2] Sami S. Zoghbi,[5] and John P. Seibyl[1,2,4]

Departments of [1]Diagnostic Radiology and [2]Psychiatry, Yale University, New Haven, CT; [3]Martha Entenmann Tinnitus Research Center, State University of New York, Brooklyn, NY; [4]Institute for Neurodegenerative Disorders, New Haven, CT; and [5]National Institutes of Mental Health, Bethesda, MD

Abstract: Tinnitus affects nearly 50 million people in the United States, with a minority demonstrating marked functional impairment. Alterations of gamma aminobutyric acid (GABA) neuronal function and benzodiazepine receptor (BZR) function in particular have been implicated in the pathophysiology of severe, chronic tinnitus. The purpose of our study was to evaluate the distribution of BZR in the brain using ^{123}I-iomazenil single-photon emission computed tomography (SPECT) imaging in patients with severe, intractable central tinnitus. Six patients with severe intractable tinnitus received a bolus and constant infusion of ^{123}I-iomazenil intravenously over 7 hours with SPECT and magnetic resonance imaging of the brain. After magnetic resonance imaging coregistration, standardized regions of interest were placed over the cerebellar, frontal (control), superior temporal, hippocampal, and thalamic regions bilaterally on (SPECT) images. Venous blood samples were drawn at specified intervals to determine equilibrium distribution volumes (V3′) for each of the regions. Variation in V3′ values in homotypic regions were calculated using a Wilcoxon signed rank test. Twelve normal control subjects were compared to the study subjects using statistical parametric mapping. Comparison of homotypic brain regions showed statistically significant asymmetry in the V3′ data in the superior temporal cortex ($p = .03$ for both). No statistically significant difference was noted in any of the other regions studied. Comparison of the group of study subjects to healthy controls revealed an insignificant trend toward reduction in BZR density in the frontal lobes bilaterally ($p = .000$) and a reduction in the cerebellum ($p = .045$). Current understanding suggests GABA receptors and the temporal lobe system as the final common pathway. This pilot study suggests possible alterations on ^{123}I-iomazenil SPECT imaging and the need for larger studies.

Key Words: brain single-photon emission computed tomography (SPECT); gamma aminobutyric acid (GABA); iomazenil; receptor imaging; Statistical Parametric Mapping (SPM); tinnitus

Tinnitus is defined as a sensory disorder of auditory perception reflecting an aberrant auditory signal produced by interference in the excitatory-inhibitory processes involved in neurotransmission [1]. The definition of tinnitus is constantly being refined as a result of the integration of information from otolaryngology, psychiatry, neurology, and nuclear medicine. Tinnitus has been attributed to peripheral abnormality in the function of the vestibulocochlear apparatus, to cranial nerve dysfunction, or to central nervous system causes. According to the American Tinnitus Association, approximately 50 million people are affected with tinnitus in the United States. Of these, approximately

Reprint requests: Aditya Daftary, MBBS, Section of Nuclear Medicine, Department of Diagnostic Radiology, 333 Cedar Street, New Haven, CT 06510. Phone: 203-785-2834; Fax: 203-688-5040; E-mail: Aditya.Daftary@yale.edu

This work was generously supported by the Martha Entenmann Tinnitus Research Center, Inc., Brooklyn, NY.

12 million have significant tinnitus, and some 2 million have tinnitus that impairs normal daily functioning (http://www.ata.org/about_tinnitus/).

Although some have speculated regarding the pathophysiological mechanisms associated with severe central-type tinnitus, little is definitively understood. Current hypotheses implicate excitatory amino acid–induced neuroexcitotoxicity and abnormal epileptiform activity [2–5]; hence, antiseizure drugs have been used in the treatment of tinnitus. The therapeutic effect of benzodiazepines in treating tinnitus was studied initially by Melding et al. [5], whose work—in conjunction with that of Lechtenburg and Shulman [2] and Collins et al. [3]—forms the basis of widespread use of these drugs clinically with some success.

^{123}I-iomazenil is a partial inverse agonist of the benzodiazepine receptor (BZR) and has been used in a number of studies evaluating the role of gamma aminobutyric acid (GABA) mechanisms in neuropsychiatric disorders [6–10]. Using a method of bolus plus constant infusion to establish equilibrium-binding kinetics in the brain allows the performance of accurate quantitative analyses of the density of BZR binding sites in the cortex. An intrasubject study comparing ^{11}C-iomazenil positron emission tomography (PET) and ^{123}I-iomazenil single-photon emission tomography (SPECT) in healthy subjects demonstrated excellent comparability of these tracers for in vivo assessment of BZR binding [11]. The purpose of our study was to apply these techniques to evaluate cortical BZR using ^{123}I-iomazenil SPECT imaging in patients with severe, central-type tinnitus as compared with healthy age-matched controls.

PATIENTS AND METHODS

Patients

The study was performed in accordance with the protocols approved by the institutional review board at the Yale University School of Medicine. Patients were recruited from the Martha Entenmann Tinnitus Research Center–Health Sciences Center, Brooklyn, State University of New York and Forest Hills, NY. The selection criteria included the following: (1) age older than 21 years; (2) medical-audiological tinnitus patient protocol (MATPP) tinnitus screening protocol to confirm central-type tinnitus [12]; (3) normal screening laboratory investigations (blood count; Na, K, Cl, HCO_3, blood urea nitrogen, creatinine, glucose, Ca, PO_4, serum glutamic-oxaloacetic transaminase, serum glutamic-pyruvic transaminase, lactic dehydrogenase, alkaline phosphatase, creatine phosphokinase, bilirubin, total protein, and albumin levels; urinalysis; and urine drug screen); and (4) normal brain magnetic resonance imaging (MRI) within 60 days of the study. Patients were excluded from the study for (1) pregnancy, (2) neurological or axis I psychiatric illness, (3) significant medical disease, (4) intake of medications known to affect GABA or BZR in 2 weeks before radiopharmaceutical administration, and (5) alcohol or psychotropic drug use within 2 weeks before the SPECT study.

Table 1. Study Subject and Control Demographics and Brief Scan Data

	Gender	Age (yr)	Time*	Total Dose (Bq)	B/I
Subject					
1	M	57.4	6:31	367.04	3.79
2	F	53.7	6:34	370.37	3.78
3	M	63.2	5:29	368.89	3.78
4	F	69.5	5:26	368.89	3.78
5	M	37.3	5:31	222	3.90
6	F	52.7	5:07	221.63	3.85
Mean		55.6	5:46	319.79	3.81
SD		10.9	0:36	75.85	0.05
COV%		0.20	0.11	0.24	0.01
Control					
1	M	52.3	6:37	220.15	3.81
2	M	53.3	6:04	222	3.87
3	M	54.9	6:07	224.96	3.82
4	M	54.9	5:46	222.37	3.81
5	M	55.8	6:14	220.52	3.81
6	M	59.5	5:45	222	3.90
7	M	39.3	6:07	219.41	3.94
8	M	35.8	5:56	224.59	3.82
9	F	46.7	5:52	194.99	3.79
10	F	50.4	6:17	222.37	3.82
11	M	50.6	6:00	222	3.90
12	M	51.3	5:52	223.48	3.82
Mean		50.4	6:03:05	219.78	3.84
SD		6.9	0:14	8.14	0.05
COV%		0.14	0.041	0.04	0.01

B/I = bolus-to-infusion ratio; COV% = coefficient of variation expressed as a percentage.
* Injection to scan time.

The study group consisted of six patients. Of these patients, two had bilateral tinnitus in the ears, two in the head only, and two in both the head and the ears. All patients were right-handed. Patient demographics are detailed in Table 1. Twelve control subjects were selected from a database of healthy controls with no lifetime psychiatric diagnosis and no clinically significant medical or neurological history, including tinnitus, on the basis of physical examination and laboratory studies.

Radiolabeling

^{123}I-iomazenil was prepared by a method previously described [13,14], with an average yield of 58.25%

(standard deviation [SD], 7.38%) and radiochemical purity of 96.7% (mean, 2.2; coefficient of variation (COV), 2.3%). Sterility was confirmed by lack of growth in fluid thioglycolate at 35° and soybean-casein digest at 25° for 2 weeks. Apyrogenicity was confirmed by the LAL test (Endosafe, Charleston, NC). All patients received potassium iodide (0.6 g SSKI solution) in the 24-hour period before the scan.

Plasma Analysis

Three venous blood samples were collected at 240, 300, and 360 minutes (means ± SD: 264 ± 25 minutes, 324 ± 21 minutes, and 369 ± 15 minutes, respectively) after starting the infusion of iomazenil, and blood samples were analyzed as previously described [14]. We chose these intervals on the basis of previous studies indicating that plasma levels of iomazenil reach steady state by these times [15]. A 500-μl aliquot of the plasma was counted to measure the total plasma activity concentration (CP_{ACT} [μCi/ml]). Metabolite-corrected parent compound plasma concentration (CP_{PAR} [μCi/ml]) was obtained after extraction with ethyl acetate and reverse-phase high-performance liquid chromatography (HPLC) and was calculated for each sample. Plasma protein binding was measured by ultrafiltration through Centrifree membrane filters (Amicon Division, WR Grace & Co, Danvers, MA) [16], and the plasma-free fraction of iomazenil (CP_{FREE} [μCi/ml]) was calculated. This procedure was repeated for each patient, and correction to the time of injection was performed. Plasma data were not available for those in the control group.

Data Acquisition

Patients received a priming bolus of ^{123}I-iomazenil (mean, 102.49 ± 24.05 MBq for cases, 71.04 ± 29.6 MBq for controls) followed by a continuous infusion of ^{123}I-iomazenil (mean, 217.19 ± 51.8 MBq for cases, 148.74 ± 5.55 MBq for controls) at a constant rate (mean, 7.47 ± 0.05 ml/hr for cases, 7.51 ± 0.02 ml/hr for controls). The duration of the infusion was 7 hours. Patient demographics and doses are summarized in Table 1. The mean bolus-to-infusion ratios were comparable to those from our previous studies, where they were shown to be optimal in achieving steady state of parent compound and unchanging time-activity curves in cortex [15]. Imaging was started on average within 345 ± 19 minutes and 363 ± 38 minutes after bolus radiotracer administration, respectively, for cases and controls. SPECT images of the cases were acquired as a single 36-minute scan. Control subject images were acquired by three serial 18-minute scans that were summed before being used in image analysis. In one control study, owing to technical difficulties, only two scans were available. Plasma data for controls were unavailable. All tinnitus patients underwent MRI and coregistration with SPECT scans (as described later) for directing region-of-interest placement.

Image Analysis

SPECT projection data were filtered with a two-dimensional low-pass filter (order = 4; cutoff frequency = 0.4 cycles per pixel) and then were transversely reconstructed with a ramp-back projection filter on a 128 × 128 matrix. Attenuation correction was performed using the Chang 0 method [17] with an attenuation μ determined empirically from a ^{123}I-containing distributed-source cylindrical phantom of approximate geometry and dimensions of the head. SPECT images were co-registered to the respective magnetic resonance images using Statistical Parametric Mapping (SPM96) [18]. An operational method for a standardized region-of-interest strategy was developed by consensus of two experienced research nuclear medicine physicians, and regions of interest were placed. The a priori hypothesis in this preliminary investigation was that chronic tinnitus would show abnormalities in the cerebellum, hippocampus, temporal lobes, and thalamic nuclei [19]. We analyzed asymmetry in these regions as an indicator of dysfunction. Regions of interest were placed on magnetic resonance images in the frontal, superior temporal, thalamic, hippocampal, and cerebellar cortices on two consecutive slices 3.56-mm thick (mean size of regions of interest was 244.953 mm^2, except cerebellar regions of interest, which were 676.914 mm^2). Adjacent slices were summed to produce volumes of interest for each region (cerebellum, 4072.02 ± 0 mm^3; hippocampus, 1468.623 ± 1.76 mm^3; superior frontal, 1468.404 ± 1.78 mm^3; temporal, 1467.963 ± 2.6 mm^3; and thalamus, 1468.624 ± 1.35 mm^3). Mean regional activity (cpm/mm^3) was calculated for each volume, corrected to the time of infusion, and expressed as becquerels per milliliter (Bq/ml) by using a calibration factor of 45.4 Bq/cpm determined from six experiments using a 12-cm-diameter cylindrical phantom containing uniformly distributed ^{123}I. The analysis was performed on the V3′ values in all volumes of interest.

Outcome Measures

The primary imaging outcome measures of this study were (1) the homotypic ratio of count density for the a priori selected brain regions, (2) the regional equilibrium distribution volume determined by the ratio of activity in brain region divided by the concentration of

parent compound, and (3) statistical parametric analysis of tinnitus patients compared with age- and gender-matched controls.

Statistical Analysis

Volume-of-Interest Analysis

This study was an intrasubject analysis in which assessment of the asymmetry in distribution of BZR in homotypic brain regions was performed. The asymmetry in the V3′ values in each of the volumes previously mentioned was compared. The variability of V3′ data in each volume of interest, when compared to the opposite side, was calculated using the Wilcoxon signed rank test.

SPM Analysis

In addition to the foregoing, a case-control strategy using SPM was employed. All patient and control images were processed as described (see the section, "Image Analysis") and then imported into a commercial image analysis program (MedX, vol. 3.4, Sensor Systems Inc., Sterling, VA). Using the SPM99 [18] realign function, a mean image was created, and images were resliced and spatially normalized to a template image in SPM standard anatomical space (Montreal Neurological Institute space) using a 10 × 10 × 12–mm Gaussian kernel. Proportional scaling of the global mean was performed using an analysis threshold of 0.8. The study group (n = 6) was compared to the control group (n = 12) using a two-sample *t*-test for areas of relative increase or decrease in radiotracer accumulation. The extent threshold (k), below which clusters were rejected, was 125 voxels, which corresponds to the approximate resolution of SPECT imaging in tissue, which is 1 mm^3. The voxel height threshold was set at 0.005, corresponding to a *Z*-score of 2.8.

Table 2. Plasma Analysis Depicting Proportions of Parent Compound and Free Parent Compound

Subject	% Parent by HPLC	Free Parent Fraction
1	96.20	30.60
2	97.20	33.90
3	96.97	37.50
4	97.73	34.70*
5	96.40	36.30
6	94.50	29.40
Mean	96.50	33.73
SD	1.03	2.90
COV%	1.06	8.59

COV% = coefficient of variation expressed as a percentage; HPLC = high-performance liquid chromatography.
* Only two plasma samples analyzed, owing to technical reasons.

Table 3. Comparison of V3′ Data in Homotypic Regions

Region	Mean Left (SD)	Mean Right (SD)	*p* Value
Cerebellum	96 (32.8)	84.6 (22.1)	0.3
Hippocampus	124 (42.7)	130 (47)	0.56
Superior temporal	142.1 (37.3)	151.5 (39.9)	0.03*
Frontal	132.5 (23.7)	132.5 (29)	0.84
Thalamus	68.2 (26.1)	75.1 (29.7)	0.22

SD = standard deviation.
* Statistically significant.

RESULTS

Plasma Analysis

The concentration of the free fraction of iomazenil in plasma was calculated at three different time points as described (except in one patient, owing to technical reasons). The plasma analysis data is summarized in Table 2. The composition of parent tracer measured by HPLC was 96.5% (SD, 1.03%), which compares well with other published data [6]. The V3′ value for the radiotracer in each region of interest was calculated using the free fraction of the parent. The fraction of free parent was 33.73% (SD, 2.9%), which compares favorably with results in other similar studies [7,8].

As regards asymmetry of radiotracer distribution in homotypic brain regions, V3′ data from the regions already described were analyzed using a Wilcoxon signed rank test. The results of paired two-tailed comparison of homotypic brain regions with raw counts and V3′ levels are described in Table 3. Variability in homotypic V3′ values is displayed in Figure 1.

Statistical analysis of volume-of-interest activity in

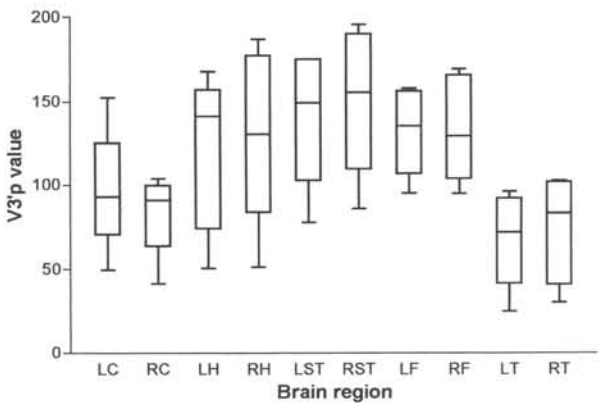

Figure 1. Variability of V3′ values in different brain regions from volume-of-interest analysis. (*L*, *R* = left, right; *C* = cerebellum; *H* = hippocampus; *ST* = superior temporal [*p* = .03]; *F* = frontal; *T* = thalamic.)

Table 4. Location and Magnitude of Areas of Significantly Decreased Receptor Density (Cluster Level)

Cluster Location	*p* Value (Corrected)	*Z*-score	Coordinates *x*, *y*, *z* (mm)
Left frontal lobe	0.000	4.84	−12, 24, 58
Right cerebellum	0.045	3.69	10, −80, −16

Note: In subjects with tinnitus when compared to healthy subjects.

homotypic regions showed statistically significant asymmetry in BZR density (expressed as V3′) in the superior temporal cortical region. The cerebellum, hippocampus, and thalamic regions did not show any significant asymmetry in receptor density (see Table 3).

SPM Analysis

Comparison of cases and controls showed a significant decrease in counts in the frontal lobes ($p = .000$) and an insignificant decrease in the cerebellum. This information is summarized in Table 4 and in Figures 2 and 3.

DISCUSSION

This study evaluated patients with severe intractable tinnitus using a bolus and constant infusion of ^{123}I-iomazenil SPECT brain imaging. We also compared the SPECT scans of these patients with scans of historically normal control subjects. To the best of our knowledge, this is the first time BZR imaging studies have

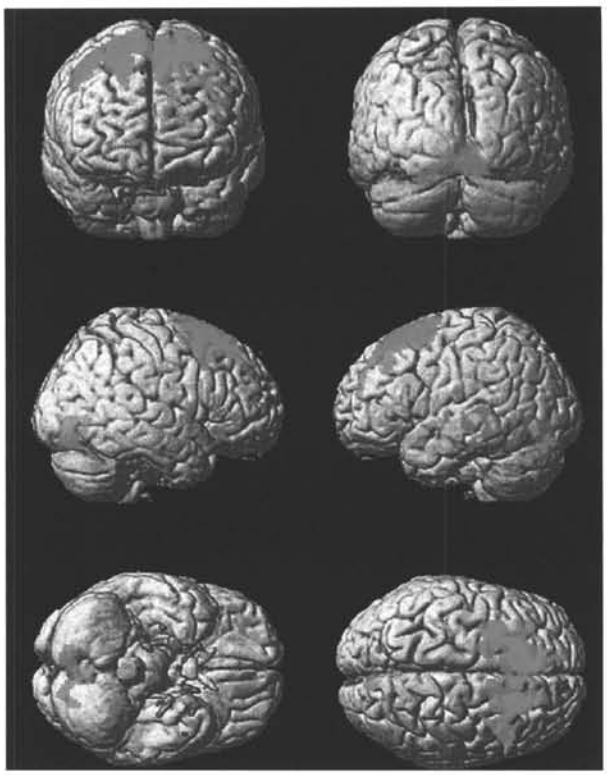

Figure 2. Results of SPM analysis depicting areas of relatively decreased counts (frontal lobe and cerebellum) (k = 125 voxels; height threshold = 0.005) in 6 tinnitus subjects as compared to 12 controls.

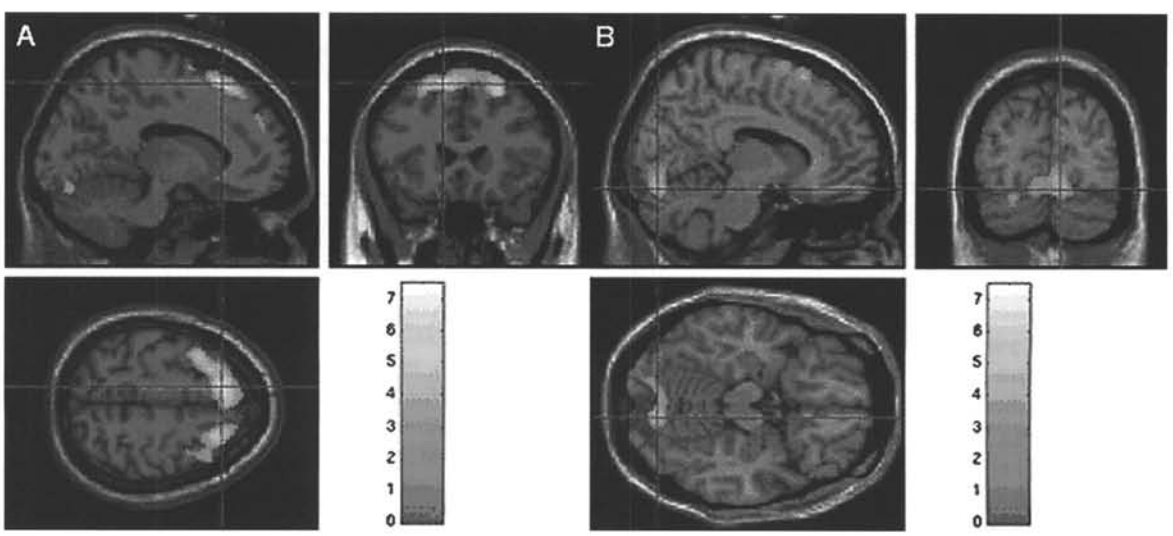

Figure 3. Cross-sectional appearance of most significant voxels in the two clusters (A, frontal; B, cerebellar) demonstrating decreased receptor density in subjects with tinnitus. Areas are overlaid on a standard T_1-weighted magnetic resonance image.

been performed on patients with severe, chronic central tinnitus.

We followed two strategies for image analysis. The first was a study of region (volume) of interest in which we collected data from brain regions that have been implicated in tinnitus [1,19–22] followed by a voxel-based SPM analysis that would not be biased by our previous concerns about specific area involvement in tinnitus.

In the first part, we analyzed asymmetry in V3′ values in each region of interest (volume of interest), findings that would enable us to identify visually detectable difference, which may assist in interpretation of these scans in the future and act as a direct measure of receptor distribution. We found that the asymmetries identified in the superior temporal region with V3′ data matched with our informal visual estimation of asymmetry.

The results of the voxel-based SPM analysis also suggest changes in BZR distribution in the frontal lobes and, to a lesser extent, in the cerebellum. The frontal lobe showed the least asymmetry; for the volume-of-interest assessment, however, this analysis does not account for the symmetrical relative reduction in frontal lobe receptor concentration. We also saw an insignificant decrease in receptor concentration in the cerebellum. The findings of this study do not correlate with the current understanding of tinnitus, which indicates a possible seat of pathology in the temporal lobes [1,19, 23,24]. At an earlier stage of this project, we noted a trend showing decreased receptor density in the right cerebellum [25]; however, since then, we have reanalyzed data with closer age matching and also using newer image-processing techniques.

Conclusions based on these data should be tempered by several issues in the study design; these include a relatively small number of patients studied, potential confound of age on BZR in the healthy control population, and effect of drug treatment on the imaging.

This was a preliminary study; hence, a limited number of patients was studied. Owing to the low number of healthy control iomazenil SPECT scans, we were unable to age- and gender-match our controls exactly to the cases. This brought up an interesting question: Were age- and gender-matching of controls actually necessary in iomazenil studies? In 16 healthy volunteers aged 21–78 years and studied with ^{11}C-RO-4513 PET, no significant change with age was seen in 10 brain regions studied [26]. Also, correlation between ^{123}I-iomazenil SPECT and ^{11}C-iomazenil PET studies has been good [11]; however, in both these studies, only a bolus injection of the tracer was performed, which does not necessarily produce equilibrium binding offered by the bolus and constant infusion method used in our study.

Multiple studies show that short-term administration of benzodiazepines produces mild to no change that reverses rapidly on cessation of therapy [6,27]. We cannot, however, exclude that these changes may be in part secondary to reduced affinity of BZR to ^{123}I-iomazenil or to changes in receptor distribution from long-term treatment of the condition with benzodiazepines.

Some studies have shown alteration in cerebral metabolism with the presence and absence of symptoms [21]. What is useful to know, however, is that at the time of the study, all these patients were suffering from tinnitus and that their symptoms had been refractory to treatment.

Finally, imaging measures of alteration in the density of BZR binding may well represent an epiphenomenon associated with tinnitus rather than the primary pathophysiological process. This study, however, should prove to be an effective method on which to base future work and improve our understanding of tinnitus, of its pathophysiology, and of monitoring treatment.

CONCLUSION

This preliminary study of BZR distribution in a cohort experiencing severe, chronic tinnitus supports temporal, frontal lobe, and cerebellar involvement in the disorder. This study is the first time that quantification of BZR has been performed on patients with severe, chronic, intractable tinnitus, and it should form a framework for some of the larger studies that could bring to bear an improved description of the natural history of the symptoms and improve treatments.

REFERENCES

1. Shulman A. A final common pathway for tinnitus—the medial temporal lobe system. *Int Tinnitus J* 1(2):115–126, 1995.
2. Lechtenberg R, Shulman A. Benzodiazepines in the treatment of tinnitus. *Arch Neurol* 41:718–721, 1984.
3. Collins RC, Dobkin BH, Choi DW. Selective vulnerability of the brain: new insights into the pathophysiology of stroke. *Ann Intern Med* 110(12):992–1000, 1989.
4. Shulman A. Neuroprotective drug therapy: A medical and pharmacological treatment for tinnitus control. *Int Tinnitus J* 3(2):77–93, 1997.
5. Melding PS, Goodey RS, Thorne PR. The use of intravenous lidocaine in the diagnosis and treatment of tinnitus. *J Laryngol Otol* 92:115–121, 1978.
6. Fujita M, et al. Changes of benzodiazepine receptors during chronic benzodiazepine administration in humans. *Eur J Pharmacol* 368(2–3):161–172, 1999.
7. Abi-Dargham A, et al. No evidence of altered in vivo benzodiazepine receptor binding in schizophrenia. *Neuropsychopharmacology* 20(6):650–661, 1999.

8. Abi-Dargham A, et al. Alterations of benzodiazepine receptors in type II alcoholic subjects measured with SPECT and [^{123}I] Iomazenil. *Am J Psychiatry* 155(11): 1550–1555, 1998.
9. Bremner JD, et al. Decreased benzodiazepine receptor binding in prefrontal cortex in combat-related posttraumatic stress disorder. *Am J Psychiatry* 157(7):1120–1126, 2000.
10. Verhoeff NP, et al. [123-I] Iomazenil SPECT benzodiazepine receptor imaging in schizophrenia. *Psychiatry Res* 91(3):163–173, 1999.
11. Bremner JD, et al. Quantitation of benzodiazepine receptor binding with PET [^{11}C] Iomazenil and SPECT [^{123}I] Iomazenil: Preliminary results of a direct comparison in healthy human subjects. *Psychiatry Res* 91(2):79–91, 1999.
12. Shulman A, et al. *Tinnitus Diagnosis/Treatment*. Philadelphia: Lea & Febiger, 1991.
13. Zea-Ponce Y, et al. Formation of 1-[^{123}I] Iodobutane in labeling [^{123}I] Iomazenil by iododestannylation: Implications for the reaction mechanism. *Appl Radiat Isot* 45(1):63–68, 1994.
14. Zoghbi SS, et al. Pharmacokinetics of the SPECT benzodiazepine receptor radioligand [^{123}I] Iomazenil in human and non-human primates. *Nucl Med Biol* 19(8):881–888, 1992.
15. Abi-Dargham A, et al. SPECT measurement of benzodiazepine receptors in human brain with iodine-123-iomazenil: Kinetic and equilibrium paradigms. *J Nucl Med* 35(2):228–238, 1994.
16. Gandelman MS, et al. Evaluation of ultrafiltration for the free-fraction determination of single photon emission computed tomography (SPECT) radiotracers: beta-CIT, IBF, and iomazenil. *J Pharm Sci* 83(7):1014–1019, 1994.
17. Chang LA. Method for attenuation correction in computed tomography. *IEEE Trans Nucl Sci* 25:638–643, 1987.
18. Friston KJ, et al. Statistical parametric maps in functional imaging: A general linear approach. *Hum Brain Map* 2:189–210, 1995.
19. Shulman A, et al. SPECT imaging of brain and tinnitus—neurotologic/neurologic implications. *Int Tinnitus J* 1(1): 13–29, 1995.
20. Mirz F, et al. Positron emission tomography of cortical centers of tinnitus. *Hear Res* 134(1–2):133–144, 1999.
21. Giraud AL, et al. A selective imaging of tinnitus. *Neuroreport* 10(1):1–5, 1999.
22. Arnold W, et al. Focal metabolic activation in the predominant left auditory cortex in patients suffering from tinnitus a PET study with [18F] deoxyglucose. *J Otorhinolaryngol* 58(4):195–199, 1996.
23. Shulman A, Goldstein B. A final common pathway for tinnitus—implications for treatment. *Int Tinnitus J* 2:137–142, 1996.
24. Shulman A, Goldstein B. Medical significance of tinnitus. *Int Tinnitus J* 3(1):45–50, 1997.
25. Shulman A, et al. Benzodiazepine receptor deficiency and tinnitus. *Int Tinnitus J* 6(2):98–111, 2000.
26. Suhara T, et al. No age-related changes in human benzodiazepine receptor binding measured by PET with [^{11}C] Ro 15-4513. *Neurosci Lett* 159(1–2):207–210, 1993.
27. Sybirska E, et al. [^{123}I] Iomazenil SPECT imaging demonstrates significant benzodiazepine receptor reserve in human and nonhuman primate brain. *Neuropharmacology* 32(7):671–680, 1993.